

Anomalous supercurrents in the presence of particle losses

Risa Ogino¹ and Shun Uchino^{1,2}

¹*Department of Materials Science, Waseda University, Tokyo 169-8555, Japan*

²*Department of Electronic and Physical Systems, Waseda University, Tokyo 169-8555, Japan*

We show that supercurrent properties in a superfluid or superconducting junction are significantly modified due to single-particle losses present in a conduction channel. In the presence of a spin-independent particle loss, we find regimes where the Josephson current $I_N(\phi)$ takes zero at a position in between $\phi = 0$ and $\phi = \pi$, and the direction of the supercurrent is reversed. Although the region is narrow, we also find a regime in which the critical current is enhanced by dissipation. Such anomalous behaviors in the Josephson current are attributed to a subtle interplay between the contribution that is present regardless of dissipation and the unconventional one that is absent without dissipation. In the presence of a spin-selective particle loss, it is shown that a dissipation-induced spin supercurrent and its reversal occur. The proposed system is analyzed by means of the Keldysh field theory approach based on the Gorini-Kossakowski-Sudershan-Lindblad master equation and may be realized in ultracold atomic gases and solid-state systems.

I. INTRODUCTION

The Josephson effect that represents a flow tunneling through a barrier without a biased voltage is an outstanding yet ubiquitous phenomenon in physics [1]. In a simple superconducting junction where an insulator is sandwiched between conventional superconductors, the DC current usually obeys

$$I = I_C \sin \phi, \quad (1)$$

with critical current I_C and relative phase between two superconductors ϕ . The Josephson effect has also been examined in superfluid Helium [2], elementary particle physics [3], and ultracold atomic gases [4]. In addition to the importance in fundamental physics, it plays a crucial role as a building block of quantum technology such as superconducting quantum interference device [5] and superconducting qubit [6].

One of the vital questions in superconducting junctions is how nonequilibrium disturbance affects the Josephson effects [7]. The prominent example is the Caldeira-Leggett model originally introduced to explain the dissipation effect in Josephson junctions. There, the Ohmic resistance in the junctions is incorporated as the coupling effect with harmonic oscillators that model an environment [8]. Another remarkable example, which is relevant to the present study, is the presence of the supercurrent reversal phenomenon where a dirty superconducting junction is driven out of equilibrium due to a coupling to a normal current [9]. The current reversal phenomenon is also known as π -junction since the current-phase relation shifts by π [10, 11]. The π -junction has originally been realized in a variety of equilibrium junctions such as ferromagnetic Josephson junction [12], Josephson junction with unconventional superconductors [13], and superconducting quantum dot [14], and has also attracted attention in terms of quantum computation such as implementation of a qubit with a long coherence time [15].

Nowadays, ultracold atomic gases provide an ideal toolbox to explore the Josephson junctions [16]. By

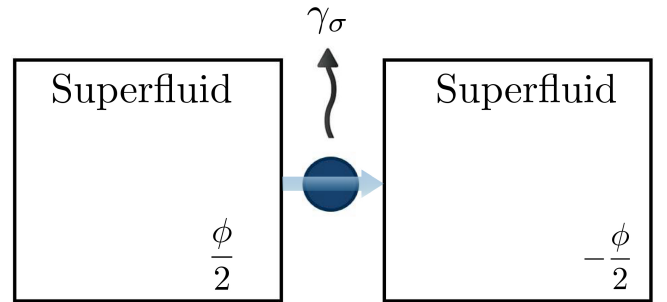


FIG. 1. Two-terminal Josephson junction system discussed in this paper. A particle current between superfluids or superconductors induced by a relative phase bias ϕ passes through a quantum dot where single particle losses occur.

controlling an interatomic interaction, one can realize fermionic superfluids whose transport properties have already been examined in mesoscopic setups such as quantum point contact [17] and junction systems [18]. Josephson current properties in such gases can also be examined through current-biased junctions, which have successfully been implemented [19–21]. Furthermore, a unique capability in ultracold atomic gases allows for dissipation control in quantum many-body systems [22]. In the context of mesoscopic transport, dissipative transport induced by a single particle loss has been measured [23]. There, a spin-selective dissipation takes place in the mesoscopic channel region in a quantum point contact and induces the disappearance of the quantized conductance. Since the similar experiment under superfluid reservoirs has also been realized with the Feshbach resonance, which showed that non-linear current-bias curves arising from the multiple Andreev reflections are weakened by dissipation [24], it would be intriguing to examine how such a dissipation affects Josephson current properties.

Another notable development in Josephson junctions is a connection with non-Hermitian physics [25]. Recent theoretical works have demonstrated that non-Hermitian effects mimicking dissipation modify the Josephson cur-

rents [26–34]. The non-Hermitian Hamiltonian naturally emerges from the non-unitary evolution term in the Gorini-Kossakowski-Sudarshan-Lindblad(GKSL) master equation [35]. At the same time, the full time evolution in the GKSL master equation also contains the so-called quantum jump term whose inclusion is required for description of generic Markovian dynamics in open quantum systems. Therefore, it is fundamentally important to look at the dissipative Josephson effects at the full GKSL level. We note that such an analysis has direct relevance to experiments of ultracold atomic gases whose dissipation effects can usually be captured within the GKSL master equation [36].

Motivated by the recent experimental progress in ultracold atomic gases and the non-Hermitian treatment of the dissipative Josephson junction, here we shed light on a mesoscopic Josephson junction system where a non-interacting quantum dot accompanied by a single particle loss is attached to two superfluid or superconducting leads (Fig. 1). We note that such a system has recently been harnessed to explain transport properties in the lossy superfluid point contact realized in ultracold atomic gases [24, 37]. By using the Keldysh formalism that allows to analyze the systems obeying the GKSL master equation in an efficient manner, we demonstrate the anomalous behaviors such as the Josephson current with extra nodes in addition to conventional ones, π -junction behavior and dissipation-enhanced critical current. In contrast to the conventional wisdom such that a dissipation nulls coherent transport, furthermore, we find emergent phenomena in which spin supercurrent and its reversal are induced in the presence of spin-selective particle loss.

The structure of the paper is as follows. In Sec. II, we adopt the field theory approach that combines the Keldysh formalism with the GKSL master equation. By applying such formalism to the superconducting junction, we obtain the Josephson current formulae that allow to discuss the dissipation effects. Section III shows numerical results of the Josephson currents in the presence of a spin-independent particle loss, as well as ones in the presence of a spin-selective particle loss. Section IV is devoted to discussion and outlook. Finally, some calculations in details on Green's functions, Dyson equation in the Keldysh formalism, and current expressions are discussed in Appendices A, B and C.

II. FORMULATION OF THE PROBLEM

To uncover prototypical roles of particle losses in Josephson junctions, we consider the system in which two superfluid or superconducting reservoirs are connected via a non-interacting quantum dot (Fig. 1). In the absence of dissipation, the evolution of the density matrix ρ is described by the von Neumann equation

$\partial_\tau \rho = -i[H, \rho]$ with the Hamiltonian

$$H = H_L + H_R + H_T + H_d, \quad (2)$$

$$H_T = \sum_\sigma t[\psi_{L,\sigma}^\dagger d_\sigma + \psi_{R,\sigma}^\dagger d_\sigma + \text{h.c.}], \quad (3)$$

$$H_d = \sum_\sigma \epsilon d_\sigma^\dagger d_\sigma. \quad (4)$$

Here, $H_{L(R)}$, H_T , and H_d are the Hamiltonian of reservoir $L(R)$, tunneling term between the reservoir and quantum dot, and quantum dot Hamiltonian, respectively. In addition, $\psi_{L(R),\sigma}$ and d_σ with $\sigma = \uparrow, \downarrow$ are respectively Fermi field operators of reservoir $L(R)$ and quantum dot, t the tunneling amplitude between reservoirs and quantum dot, ϵ the onsite energy in the dot [38]. Notice that we adopt units of $\hbar = k_B = 1$. In the presence of a single particle loss at the dot, the system no longer experiences the unitary evolution and instead is described by the following quantum master equation [35]:

$$\partial_\tau \rho = -i[H, \rho] + \sum_\sigma \gamma_\sigma \left(d_\sigma \rho d_\sigma^\dagger - \frac{\{d_\sigma^\dagger d_\sigma, \rho\}}{2} \right), \quad (5)$$

where γ_σ represents the particle loss rate.

Based on this setup and taking the convention that a current is positive when particles flow from left to right reservoirs, one can determine a particle (spin) current between reservoirs $I_N(I_S)$ as follows [24, 37, 39]:

$$I_{N(S)} = \text{Re} \left[it \{ \langle \psi_{R,\uparrow}^\dagger d_\uparrow \rangle - \langle \psi_{L,\uparrow}^\dagger d_\uparrow \rangle \} \right. \\ \left. + (-)it \{ \langle \psi_{R,\downarrow}^\dagger d_\downarrow \rangle - \langle \psi_{L,\downarrow}^\dagger d_\downarrow \rangle \} \right]. \quad (6)$$

We point out that although the expression above is formally equivalent to one without dissipation, the average above $\langle \cdot \rangle$ is taken with the density matrix satisfying Eq. (5) and therefore contains effects of dissipation entirely.

In what follows, we examine behaviors of Eq. (6) in the presence of a relative phase bias between fermionic superfluid reservoirs. To this end, we adopt the Keldysh formalism, which allows to analyze observables in nonequilibrium [40] and open quantum systems [41]. In addition, we treat the Fermi superfluid in each reservoir within the mean-field theory, which has been used to compare with cold-atom experiments in Ref. [17, 24].

In order to relate the average currents with quantities calculable from the Keldysh formalism, we define the Keldysh components of Green's functions between reservoirs and quantum dot (see also Appendix A)

$$\hat{G}_{dL(R)}^K(\tau, \tau') = -i \langle [\hat{d}(\tau), \hat{\psi}_{L(R)}^\dagger(\tau')] \rangle, \quad (7)$$

$$\hat{G}_{L(R)d}^K(\tau, \tau') = -i \langle [\hat{\psi}_{L(R)}(\tau), \hat{d}^\dagger(\tau')] \rangle. \quad (8)$$

Here we introduce the following Nambu spinors of the fermionic fields [42]:

$$\hat{\psi}_{L(R)} = \begin{pmatrix} \psi_{\uparrow,L(R)} \\ \psi_{\downarrow,L(R)} \end{pmatrix}, \quad \hat{d} = \begin{pmatrix} d_\uparrow \\ d_\downarrow \end{pmatrix}, \quad (9)$$

which provides useful expressions in fermionic superfluids that exist nonzero anomalous averages such as $\langle\psi_\uparrow\psi_\downarrow\rangle$. By using above, $I_N(I_S)$ is rewritten as

$$I_N = \frac{1}{4}\text{Tr}\left[\hat{\sigma}_z\hat{t}^\dagger\hat{G}_{dL}^K(\tau,\tau) - \hat{\sigma}_z\hat{t}\hat{G}_{Ld}^K(\tau,\tau) - \hat{\sigma}_z\hat{t}\hat{G}_{dR}^K(\tau,\tau) + \hat{\sigma}_z\hat{t}^\dagger\hat{G}_{Rd}^K(\tau,\tau)\right], \quad (10)$$

$$I_S = \frac{1}{4}\text{Tr}\left[\hat{t}^\dagger\hat{G}_{dL}^K(\tau,\tau) - \hat{t}\hat{G}_{Ld}^K(\tau,\tau) - \hat{t}\hat{G}_{dR}^K(\tau,\tau) + \hat{t}^\dagger\hat{G}_{Rd}^K(\tau,\tau)\right], \quad (11)$$

where

$$\hat{t} = \begin{pmatrix} te^{-i\phi/4} & 0 \\ 0 & -te^{i\phi/4} \end{pmatrix}, \quad (12)$$

$$\hat{\sigma}_z = \begin{pmatrix} 1 & 0 \\ 0 & -1 \end{pmatrix}, \quad (13)$$

and the trace is taken for the Nambu space. Thus, it follows that the average currents are determined once Eqs (7) and (8) are calculated.

As shown in Appendices B and C, Eqs (7) and (8) can systematically be analyzed with the Dyson equation in the Keldysh formalism. Such an analysis reveals that I_N is given by

$$I_N = I_{N,c} + I_{N,uc}. \quad (14)$$

Here $I_{N,c}$ is the contribution that exists even in the absence of dissipation, and $I_{N,uc}$ is the unconventional contribution that only emerges in the presence of dissipation. Furthermore, the similar analysis for I_S leads to

$$I_S = I_{S,uc}, \quad (15)$$

where $I_{S,uc}$ represents the unconventional contribution that emerges in the presence of spin-selective dissipation. The absence of the conventional contribution in the spin current is attributed to the fact that the spin current is not usually generated by the phase bias yet is allowed owing to the spin-dependent particle loss.

III. RESULT

We now examine behaviors of the particle and spin currents at zero temperature ($T = 0$) where the maximum supercurrent is expected.

In the absence of dissipation, the phase-dependent particle current is known to be carried by the Andreev bound state and continuum contributions above the superconducting gap Δ [43]. When the resonance width $\Gamma = 2t^2/W$, where $W = 1/(\pi\rho)$ and ρ is the density of states at the Fermi energy, is much larger than Δ , the supercurrent is carried mostly by the Andreev bound states.

When Γ is smaller than Δ , in contrast, the supercurrent is dominated by the continuum contribution.

In addition, the channel transmission at the Fermi energy [43]

$$\mathcal{T} = \frac{1}{1 + (\epsilon/\Gamma)^2} \quad (16)$$

is also the key parameter for characterizing shape and amplitude of the supercurrent.

In what follows, we demonstrate how the supercurrent properties are modified in the presence of spin-independent and spin-selective particle losses at different Γ/Δ and \mathcal{T} .

A. Spin-independent particle loss case

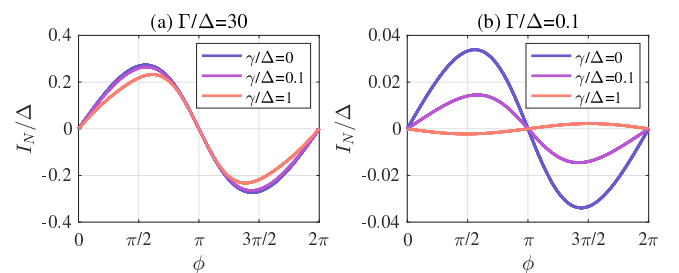


FIG. 2. Supercurrent as a function of the relative phase ϕ in different dissipation strengths. The transmission parameter is fixed to $\mathcal{T} = 0.5$. (a) $\Gamma/\Delta = 30$ and (b) $\Gamma/\Delta = 0.1$.

Here we demonstrate the supercurrent properties under the situation where up and down fermions are subject to the influence of the same dissipation, i.e., $\gamma \equiv \gamma_\uparrow = \gamma_\downarrow$.

Figure 2 (a) shows the typical phase-dependent particle current behavior at $\Gamma/\Delta \gg 1$. As increasing the dissipation strength, the current decreases monotonically. We note that such a behavior is similar to the tendency with increasing temperature, which plays a role of washing out coherent transport such as effects of the Andreev bound states.

In contrast, Fig. 2 (b) shows the supercurrent behavior at $\Gamma/\Delta \lesssim 1$. Although the current amplitude is shown to decrease as increasing dissipation, which resembles the $\Gamma/\Delta \gg 1$ case, it is remarkable that the current at $\gamma/\Delta = 1$ acquires negative values in $0 < \phi < \pi$ and positive values in $\pi < \phi < 2\pi$. The presence of the reversal of the supercurrent or π -junction is a unique feature that is present at $\Gamma/\Delta \lesssim 1$.

Figure 3 represents the presence of the current reverse phenomenon from another angle. As shown in Eq. (14), the particle current is decomposed into conventional and unconventional contributions. The conventional contribution $I_{N,c}$ monotonically diminishes as enhancing γ (Fig. 3 (a)). On the other hand, $I_{N,uc}$ that is absent without dissipation shows a non-monotonic behavior in that $I_{N,uc}$ increases and then decreases with increasing γ

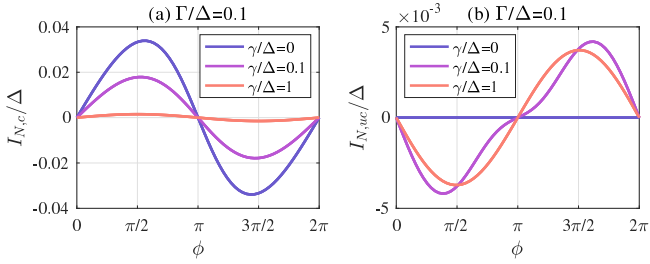


FIG. 3. Typical behaviors of $I_{N,c}$ and $I_{N,uc}$ contributions in different dissipation strengths. As in the case of Fig. 2, $\mathcal{T} = 0.5$.

(Fig. 3 (b)). It is also remarkable that $I_{N,uc}$ is opposite in sign to $I_{N,c}$. Thus, it turns out that the presence of the π -junction property is attributed to the competition between two contributions.

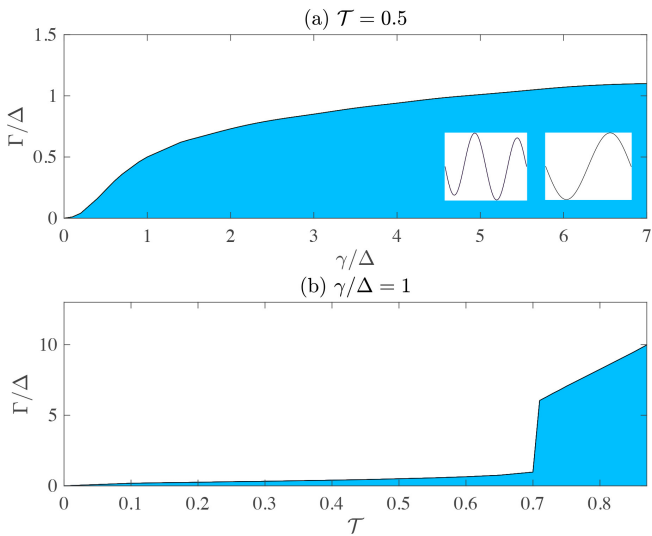


FIG. 4. Phase diagram of the dissipative supercurrent while fixing (a) $\mathcal{T} = 0.5$ and (b) $\gamma/\Delta = 1$. The figures inset show typical anomalous behaviors in the current-phase relation, which emerge in the blue regions in the phase diagrams.

Figures 4 (a) and (b) show phase diagrams of the particle current while fixing \mathcal{T} and with γ/Δ , respectively. In blue regions of both phase diagrams, we found anomalous behaviors of the supercurrent in that the π -junction or the current phase relation with multi nodes in $0 < \phi < 2\pi$ is present. What is plotted in Fig. 4 (a) is consistent with Figs. 2 and 3, since the supercurrent at $\Gamma/\Delta \gg 1$ is dominated by $I_{N,c}$ that monotonically decreases with increasing γ and does not show anomalous behaviors unlike $I_{N,uc}$. Furthermore, Fig. 4 (b) suggests that the higher transmission supports anomalous behaviors of the supercurrent.

Finally, Fig. 5 plots the critical current I_C as a function of γ at $\Gamma/\Delta = 1$ and $\mathcal{T} = 0.1$. The unique feature compared with the previous plots is its non-monotonic behavior. Namely, we found the regime in which the

critical current rather increases with increasing the dissipation strength and takes a maximum in the vicinity of $\gamma/\Delta = 1$. Such a behavior arises due to an interplay that while $I_{N,c}$ monotonically decreases with increasing γ , $I_{N,uc}$ exhibits the non-monotonic behavior and can enhance the supercurrent depending on values of γ . We also note that the non-monotonic supercurrent behavior does not always emerge yet is present around $\Gamma/\Delta = 1$ and $\mathcal{T} = 0.1$.

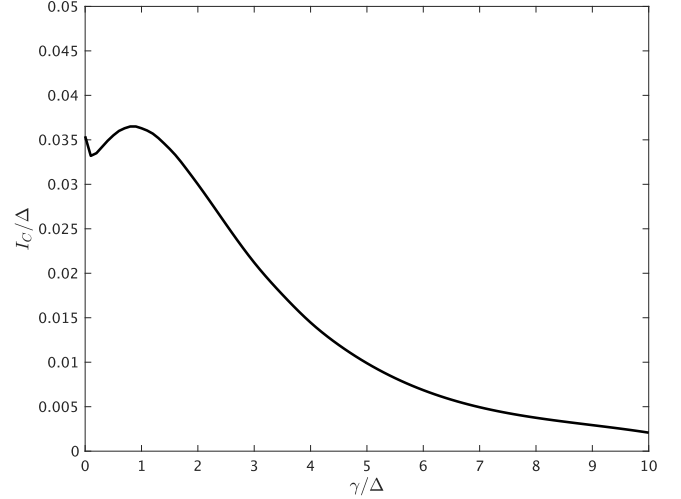


FIG. 5. Critical current I_C at $\Gamma/\Delta = 1$ and $\mathcal{T} = 0.1$ as a function of γ/Δ .

B. Spin-selective particle loss case

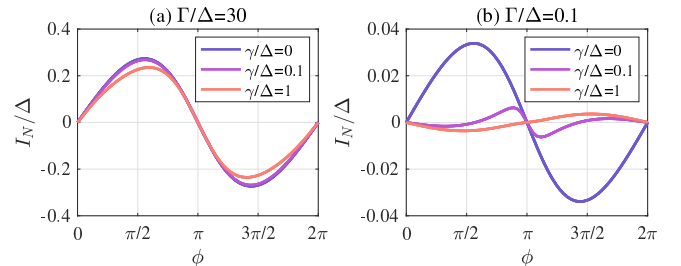


FIG. 6. Particle current in the presence of spin-selective particle loss at $\mathcal{T} = 0.5$. (a) $\Gamma/\Delta = 30$ and (b) $\Gamma/\Delta = 0.1$.

We now move on to the spin-dependent dissipation. For the sake of simplicity, we analyze the situation of $\gamma \equiv \gamma_\uparrow$ and $\gamma_\downarrow = 0$.

1. Particle current

Figure 6 shows the current-phase relation in different dissipation strengths at (a) $\Gamma/\Delta \gg 1$ and at (b) $\Gamma/\Delta \lesssim 1$. The overall tendencies are similar to those in $\gamma_\uparrow = \gamma_\downarrow$ case

in the sense that for $\Gamma/\Delta \gg 1$ the supercurrent monotonically decreases with increasing γ while the anomalous supercurrent behaviors are obtained for $\Gamma/\Delta \lesssim 1$.

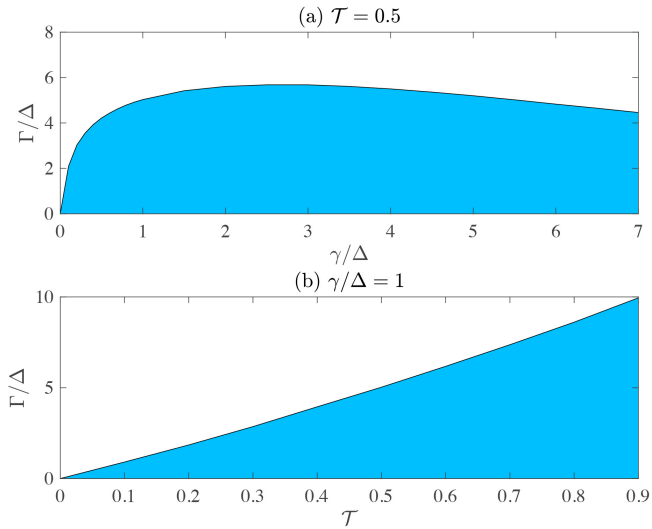


FIG. 7. Phase diagrams of the particle current at (a) constant transmission ($\mathcal{T} = 0.5$) and (b) constant dissipation strength ($\gamma/\Delta = 1$).

Figures 7 (a) and (b) show phase diagrams of the particle current with fixing \mathcal{T} and with γ/Δ , respectively. Although in common with Fig. 4 (a), the anomalous supercurrent regime increases with increasing γ , it rather decreases for $\gamma/\Delta \geq 2$. On the other hand, with increasing \mathcal{T} , the anomalous regime increases monotonically, which is consistent with Fig. 4 (b).

2. Spin current

Owing to the spin asymmetric dissipation, one can obtain a nonzero spin current by introducing a phase bias. As shown in Eq. (15), such a dissipation-induced spin supercurrent originates from the unconventional contribution.

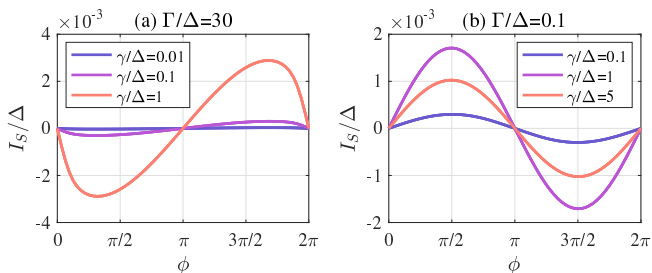


FIG. 8. Spin current in the presence of spin-dependent dissipation at $\mathcal{T} = 0.5$. (a) $\Gamma/\Delta = 30$ and (b) $\Gamma/\Delta = 0.1$.

Figure 8 shows the resultant spin currents. For $\Gamma/\Delta \gg 1$ case (Fig. 8 (a)), the induced spin current-phase relation is normal in that the current is negative for $0 <$

$\Delta\phi < \pi$ and positive for $\pi < \Delta\phi < 2\pi$. Such a behavior is interpreted that the flow of up-spin particles is hindered by the dissipation while that of down-spin particles remains unaffected. For $\Gamma/\Delta \lesssim 1$ case (Fig. 8 (b)), in contrast, we find that the spin current-phase relation becomes reverse, that is, the π -junction property for the spin current comes out. As further increasing γ , the generated spin current is reduced, which can be interpreted that phase coherent transport is eventually washed out by the dissipation.

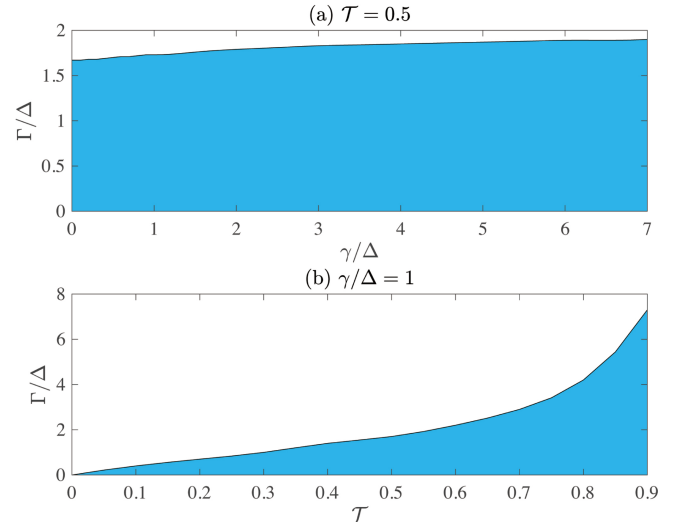


FIG. 9. Phase diagrams of the spin supercurrent at (a) $\mathcal{T} = 0.5$ and (b) $\gamma/\Delta = 1$.

Figures 9 (a) and (b) show the phase diagrams of the spin supercurrent. As in the case of the particle current, the anomalous regime is enhanced for high \mathcal{T} . In contrast, the phase boundary between normal and anomalous regimes monotonically increases with increasing γ .

IV. DISCUSSION AND OUTLOOK

Inspired by the recent experimental progress of ultracold atomic gases and non-Hermitian Josephson junctions, we have demonstrated anomalous Josephson transport through a lossy quantum dot. In the presence of spin-independent particle loss, we have demonstrated regimes where $I_N(\phi)$ crosses the horizontal axis and takes negative values for $0 < \phi < \pi$, and dissipation-enhanced critical current occurs. On top of that, the spin-selective control of dissipation, as available in cold-atom experiments, leads to the spin supercurrent phenomenon present in the dissipative regime where the strength of loss rate is intermediate.

While our predictions can naturally be designed in the cold-atom experiment, one may obtain similar result in condensed matter. For instance, one can consider a three terminal system where a mesoscopic sample is attached to two superconducting leads and one normal lead [39,

44, 45]. Then, the effect of the single particle loss may be mimicked in a situation that the chemical potential of the normal lead is much lower than that of the sample, where a particle gain from the normal lead can be ignored. The spin-selective dissipation may also be designed with the ferromagnetic junction [46] or junction with spin-orbit interactions [47]

We have discussed dissipation-induced emergent phenomena in simple mesoscopic systems. Interesting perspectives are stability against the number of sites in the channel, a correlation effect in a mesoscopic regime where connections to the Kondo effect and Tomonaga-Luttinger

liquid are anticipated, and application to bosonic superfluids, which has been realized in the Josephson junction array [48].

ACKNOWLEDGMENT

We thank T. Giamarchi and A.-M. Visuri for support in the early stage of this work. We are also grateful to T. Esslinger, P. Fabritius, M.-Z. Huang, K. Kobayashi, J. Mohan, A. F. Morpurgo, M. Talebi, and S. Wili for discussions. SU is supported by JST PRESTO (JP-MJPR235) and JSPS KAKENHI (JP25K07191).

Appendix A: Green's function

The Keldysh components of real-time Green's functions between reservoir and dot are given by Eq. (7) and Eq. (8). Similarly, real-time Green's functions at a quantum dot are expressed as

$$\hat{G}_d^R(\tau, \tau') = -i\theta(\tau - \tau')\langle\{\hat{d}(\tau), \hat{d}^\dagger(\tau')\}\rangle, \quad (\text{A1})$$

$$\hat{G}_d^A(\tau, \tau') = i\theta(\tau' - \tau)\langle\{\hat{d}(\tau), \hat{d}^\dagger(\tau')\}\rangle, \quad (\text{A2})$$

$$\hat{G}_d^K(\tau, \tau') = -i\theta(\tau - \tau')\langle[\hat{d}(\tau), \hat{d}^\dagger(\tau')]\rangle. \quad (\text{A3})$$

We now obtain the current expression induced by the phase gradient between reservoirs. By using the so-called Langreth rule [49], we can obtain the following relations for Green's functions in frequency space [50]:

$$\hat{G}_{\sigma,dL}^K(\omega) = \hat{G}_d^R(\omega)\hat{t}\hat{g}_L^K(\omega) + \hat{G}_d^K(\omega)\hat{t}\hat{g}_L^A(\omega), \quad (\text{A4})$$

$$\hat{G}_{\sigma,Ld}^K(\omega) = \hat{g}_L^R(\omega)\hat{t}^\dagger\hat{G}_d^K(\omega) + \hat{g}_L^K(\omega)\hat{t}^\dagger\hat{G}_d^A(\omega), \quad (\text{A5})$$

$$\hat{G}_{\sigma,dR}^K(\omega) = \hat{G}_d^R(\omega)\hat{t}^\dagger\hat{g}_R^K(\omega) + \hat{G}_d^K(\omega)\hat{t}^\dagger\hat{g}_R^A(\omega), \quad (\text{A6})$$

$$\hat{G}_{\sigma,Rd}^K(\omega) = \hat{g}_R^R(\omega)\hat{t}\hat{G}_d^K(\omega) + \hat{g}_R^K(\omega)\hat{t}\hat{G}_d^A(\omega). \quad (\text{A7})$$

Here, we introduce uncoupled retarded (advanced) Green's function in each reservoir $\hat{g}_{L(R)}^R(\omega)$ that does not incorporate tunneling effects between reservoirs and quantum dot. For superconducting reservoirs, it is given by [42]

$$\begin{aligned} \hat{g}_{L(R)}^{R(A)}(\omega) &\equiv \frac{1}{W} \begin{pmatrix} g^{R(A)}(\omega) & f^{R(A)}(\omega) \\ f^{R(A)}(\omega) & g^{R(A)}(\omega) \end{pmatrix} \\ &= \frac{1}{W} \begin{pmatrix} -\frac{\omega \pm i0^+}{\sqrt{\Delta^2 - (\omega \pm i0^+)^2}} & \frac{\Delta}{\sqrt{\Delta^2 - (\omega \pm i0^+)^2}} \\ \frac{\Delta}{\sqrt{\Delta^2 - (\omega \pm i0^+)^2}} & -\frac{\omega \pm i0^+}{\sqrt{\Delta^2 - (\omega \pm i0^+)^2}} \end{pmatrix}. \end{aligned} \quad (\text{A8})$$

Since each reservoir is in equilibrium, the uncoupled Keldysh component is determined via the fluctuation-dissipation theorem [40] as follows:

$$\hat{g}_{L(R)}^K(\omega) = \left[\hat{g}_{L(R)}^R(\omega) - \hat{g}_{L(R)}^A(\omega) \right] [1 - 2n(\omega)], \quad (\text{A9})$$

where $n(\omega) = \frac{1}{e^{\omega/T} + 1}$ is the Fermi distribution function. We next look at uncoupled Green's function in the quantum dot. In the presence of the dissipation, inverse Green's functions are determined as [24]

$$\begin{aligned} [\hat{g}_d^{-1}(\omega)]^R &= \begin{pmatrix} \omega - \epsilon + i\gamma_\uparrow & 0 \\ 0 & \omega + \epsilon + i\gamma_\downarrow \end{pmatrix}, \\ [\hat{g}_d^{-1}(\omega)]^A &= \begin{pmatrix} \omega - \epsilon - i\gamma_\uparrow & 0 \\ 0 & \omega + \epsilon - i\gamma_\downarrow \end{pmatrix}, \\ [\hat{g}_d^{-1}(\omega)]^K &= \begin{pmatrix} 2i\gamma_\uparrow & 0 \\ 0 & -2i\gamma_\downarrow \end{pmatrix}. \end{aligned} \quad (\text{A10})$$

Thus, uncoupled Green's functions are obtained as

$$\hat{g}_d^R(\omega) = \begin{pmatrix} \frac{1}{\omega - \epsilon + i\gamma_\uparrow} & 0 \\ 0 & \frac{1}{\omega + \epsilon + i\gamma_\downarrow} \end{pmatrix}, \quad (\text{A11})$$

$$\hat{g}_d^A(\omega) = \begin{pmatrix} \frac{1}{\omega - \epsilon - i\gamma_\uparrow} & 0 \\ 0 & \frac{1}{\omega + \epsilon - i\gamma_\downarrow} \end{pmatrix}, \quad (\text{A12})$$

$$\hat{g}_d^K(\omega) = -\hat{g}_d^R(\omega) [\hat{g}_d^{-1}(\omega)]^K \hat{g}_d^A(\omega) = \begin{pmatrix} -\frac{2i\gamma_\uparrow}{(\omega - \epsilon)^2 + \gamma_\uparrow^2} & 0 \\ 0 & \frac{2i\gamma_\downarrow}{(\omega + \epsilon)^2 + \gamma_\downarrow^2} \end{pmatrix}. \quad (\text{A13})$$

Appendix B: Dyson equation

Since uncoupled Green's functions are determined, we turn to analyze the full Green's functions in the quantum dot G_d , obeying the following the Dyson equation [50]:

$$\hat{G}_d(\omega) = \hat{g}_d(\omega) + \hat{g}_d(\omega) \hat{\Sigma}(\omega) \hat{G}_d(\omega) = \hat{g}_d(\omega) + \hat{G}_d(\omega) \hat{\Sigma}(\omega) \hat{g}_d(\omega), \quad (\text{B1})$$

where $\hat{\Sigma}(\omega)$ is the self-energy. We first look at the Dyson equation of the retarded and advanced components:

$$\hat{G}_d^{R(A)}(\omega) = \hat{g}_d^{R(A)}(\omega) + \hat{g}_d^{R(A)}(\omega) \hat{\Sigma}^{R(A)}(\omega) \hat{G}_d^{R(A)}(\omega), \quad (\text{B2})$$

where

$$\begin{aligned} \hat{\Sigma}^{R(A)}(\omega) &= \hat{t} \hat{g}_L^{R(A)}(\omega) \hat{t}^\dagger + \hat{t}^\dagger \hat{g}_R^{R(A)}(\omega) \hat{t} \\ &= \frac{\Gamma}{2} \begin{pmatrix} g_L^{R(A)}(\omega) + g_R^{R(A)}(\omega) & -e^{-i\phi/2} f_L^{R(A)}(\omega) - e^{i\phi/2} f_R^{R(A)}(\omega) \\ -e^{i\phi/2} f_L^{R(A)}(\omega) - e^{-i\phi/2} f_R^{R(A)}(\omega) & g_L^{R(A)}(\omega) + g_R^{R(A)}(\omega) \end{pmatrix}. \end{aligned} \quad (\text{B3})$$

The above Dyson equation can also be rewritten as follows:

$$\left[\hat{G}_d^{R(A)}(\omega) \right]^{-1} = \left[\hat{g}_d^{R(A)}(\omega) \right]^{-1} - \hat{\Sigma}^{R(A)}(\omega). \quad (\text{B4})$$

On the other hand, the Dyson equation of the Keldysh component is given by

$$\hat{G}_d^K(\omega) = \left[1 + \hat{G}_d^R(\omega) \hat{\Sigma}^R(\omega) \right] \hat{g}_d^K(\omega) \left[1 + \hat{\Sigma}^A(\omega) \hat{G}_d^A(\omega) \right] + \hat{G}_d^R(\omega) \hat{\Sigma}^K(\omega) \hat{G}_d^A(\omega). \quad (\text{B5})$$

Here

$$\begin{aligned} \hat{\Sigma}^K(\omega) &= \hat{t} \hat{g}_L^K(\omega) \hat{t}^\dagger + \hat{t}^\dagger \hat{g}_R^K(\omega) \hat{t} \\ &= \left[\hat{\Sigma}^R(\omega) - \hat{\Sigma}^A(\omega) \right] [1 - 2n(\omega)] \\ &= \left[[\hat{g}_d^R(\omega)]^{-1} - [\hat{g}_d^A(\omega)]^{-1} \right] [1 - 2n(\omega)] - \left[[\hat{G}_d^R(\omega)]^{-1} - [\hat{G}_d^A(\omega)]^{-1} \right] [1 - 2n(\omega)]. \end{aligned} \quad (\text{B6})$$

By using above and the Dyson equation for $G_d^{R(A)}$, \hat{G}_d^K is rewritten as

$$\begin{aligned} \hat{G}_d^K(\omega) &= \hat{G}_d^R(\omega) [\hat{g}_d^R(\omega)]^{-1} \hat{g}_d^K(\omega) [\hat{g}_d^A(\omega)]^{-1} \hat{G}_d^A(\omega) + \hat{G}_d^R(\omega) \hat{\Sigma}_d^K(\omega) \hat{G}_d^A(\omega) \\ &= -\hat{G}_d^R(\omega) [\hat{g}_d^{-1}(\omega)]^K \hat{G}_d^A(\omega) + \hat{G}_d^R(\omega) \left[\hat{\Sigma}^R(\omega) - \hat{\Sigma}^A(\omega) \right] \hat{G}_d^A(\omega) [1 - 2n(\omega)] \\ &= -\hat{G}_d^R(\omega) [\hat{g}_d^{-1}(\omega)]^K \hat{G}_d^A(\omega) + \left[\hat{G}_d^R(\omega) - \hat{G}_d^A(\omega) \right] [1 - 2n(\omega)] \\ &\quad + \hat{G}_d^R(\omega) \left[[\hat{g}_d^R(\omega)]^{-1} - [\hat{g}_d^A(\omega)]^{-1} \right] \hat{G}_d^A(\omega) [1 - 2n(\omega)]. \end{aligned} \quad (\text{B7})$$

Appendix C: Particle and spin currents

By means of the Dyson equations obtained above, the particle current I_N is expressed as

$$\begin{aligned}
I_N &= - \int \frac{d\omega}{8\pi} \text{Tr} \left[-\hat{\sigma}_z \hat{t}^\dagger \{ \hat{G}_d^R \hat{t} \hat{g}_L^K + \hat{G}_d^K \hat{t} \hat{g}_L^A \} + \hat{\sigma}_z \hat{t} \{ \hat{g}_L^R \hat{t}^\dagger \hat{G}_d^K + \hat{g}_L^K \hat{t}^\dagger \hat{G}_d^A \} \right. \\
&\quad \left. + \hat{\sigma}_z \hat{t} \{ \hat{G}_d^R \hat{t}^\dagger \hat{g}_R^K + \hat{G}_d^K \hat{t}^\dagger \hat{g}_R^A \} \hat{t} - \hat{\sigma}_z \hat{t}^\dagger \{ \hat{g}_R^R \hat{t} \hat{G}_d^K + \hat{g}_R^K \hat{t} \hat{G}_d^A \} \right] \\
&= I_{N,c} + I_{N,uc},
\end{aligned} \tag{C1}$$

where

$$\begin{aligned}
I_{N,c} &= - \int \frac{d\omega}{8\pi} \text{Tr} \left[-\hat{\sigma}_z \hat{t}^\dagger [\hat{G}_d^R \hat{t} \hat{g}_L^R - \hat{G}_d^A \hat{t} \hat{g}_L^A] + \hat{\sigma}_z \hat{t} [\hat{g}_L^R \hat{t}^\dagger \hat{G}_d^R - \hat{g}_L^A \hat{t}^\dagger \hat{G}_d^A] \right. \\
&\quad \left. + \hat{\sigma}_z \hat{t}^\dagger [\hat{G}_d^R \hat{t}^\dagger \hat{g}_R^R - \hat{G}_d^A \hat{t}^\dagger \hat{g}_R^A] - \hat{\sigma}_z \hat{t}^\dagger [\hat{g}_R^R \hat{t} \hat{G}_d^R - \hat{g}_R^A \hat{t} \hat{G}_d^A] \right] [1 - 2n(\omega)],
\end{aligned} \tag{C2}$$

$$\begin{aligned}
I_{N,uc} &= - \int \frac{d\omega}{8\pi} \text{Tr} \left[\hat{\sigma}_z \hat{t}^\dagger \hat{G}_d^R(\omega) [\hat{g}_d^{-1}(\omega)]^K \hat{G}_d^A(\omega) \hat{t} \hat{g}_L^A - \hat{\sigma}_z \hat{t} \hat{g}_L^R \hat{t}^\dagger \hat{G}_d^R(\omega) [\hat{g}_d^{-1}(\omega)]^K \hat{G}_d^A(\omega) \right. \\
&\quad \left. - \hat{\sigma}_z \hat{t} \hat{G}_d^R(\omega) [\hat{g}_d^{-1}(\omega)]^K \hat{G}_d^A(\omega) \hat{t}^\dagger \hat{g}_R^A + \hat{\sigma}_z \hat{t}^\dagger \hat{g}_R^R \hat{t} \hat{G}_d^R(\omega) [\hat{g}_d^{-1}(\omega)]^K \hat{G}_d^A(\omega) \right] \\
&\quad - \frac{1}{2} \text{Tr} \left[-\hat{\sigma}_z \hat{t}^\dagger \hat{G}_d^R(\omega) ([\hat{g}_d^R(\omega)]^{-1} - [\hat{g}_d^A(\omega)]^{-1}) \hat{G}_d^A(\omega) \hat{t} \hat{g}_L^A + \hat{\sigma}_z \hat{t} \hat{g}_L^R \hat{t}^\dagger \hat{G}_d^R(\omega) ([\hat{g}_d^R(\omega)]^{-1} - [\hat{g}_d^A(\omega)]^{-1}) \hat{G}_d^A(\omega) \right. \\
&\quad \left. + \hat{\sigma}_z \hat{t} \hat{G}_d^R(\omega) ([\hat{g}_d^R(\omega)]^{-1} - [\hat{g}_d^A(\omega)]^{-1}) \hat{G}_d^A(\omega) \hat{t}^\dagger \hat{g}_R^A - \hat{\sigma}_z \hat{t}^\dagger \hat{g}_R^R \hat{t} \hat{G}_d^R(\omega) ([\hat{g}_d^R(\omega)]^{-1} - [\hat{g}_d^A(\omega)]^{-1}) \hat{G}_d^A(\omega) \right] [1 - 2n(\omega)].
\end{aligned} \tag{C3}$$

We point out that in the limit of $\gamma \rightarrow 0$ and $\Gamma/\Delta \gg 1$, the expression above reduces to the Andreev current I_{ABS} , that is,

$$\begin{aligned}
I_N &\rightarrow I_{\text{ABS}} \\
&= \frac{\mathcal{T} \Delta^2 \sin \phi}{2E_{\text{ABS}}} \tanh \left(\frac{E_{\text{ABS}}}{2T} \right),
\end{aligned} \tag{C4}$$

where

$$E_{\text{ABS}} = \Delta \sqrt{1 - \mathcal{T} \sin^2(\phi/2)} \tag{C5}$$

is the so-called Andreev bound-state energy.

On the other hand, the spin current between reservoirs I_S is expressed as

$$I_S = I_{S,c} + I_{S,uc}, \tag{C6}$$

where

$$\begin{aligned}
I_{S,c} &= - \int \frac{d\omega}{8\pi} \text{Tr} \left[-\hat{t}^\dagger [\hat{G}_d^R \hat{t} \hat{g}_L^R - \hat{G}_d^A \hat{t} \hat{g}_L^A] + \hat{t} [\hat{g}_L^R \hat{t}^\dagger \hat{G}_d^R - \hat{g}_L^A \hat{t}^\dagger \hat{G}_d^A] \right. \\
&\quad \left. + \hat{t} [\hat{G}_d^R \hat{t}^\dagger \hat{g}_R^R - \hat{G}_d^A \hat{t}^\dagger \hat{g}_R^A] - \hat{t}^\dagger [\hat{g}_R^R \hat{t} \hat{G}_d^R - \hat{g}_R^A \hat{t} \hat{G}_d^A] \right] [1 - 2n(\omega)],
\end{aligned} \tag{C7}$$

$$\begin{aligned}
I_{S,uc} &= - \int \frac{d\omega}{8\pi} \text{Tr} \left[\hat{t}^\dagger \hat{G}_d^R(\omega) [\hat{g}_d^{-1}(\omega)]^K \hat{G}_d^A(\omega) \hat{t} \hat{g}_L^A - \hat{t} \hat{g}_L^R \hat{t}^\dagger \hat{G}_d^R(\omega) [\hat{g}_d^{-1}(\omega)]^K \hat{G}_d^A(\omega) \right. \\
&\quad \left. - \hat{t} \hat{G}_d^R(\omega) [\hat{g}_d^{-1}(\omega)]^K \hat{G}_d^A(\omega) \hat{t}^\dagger \hat{g}_R^A + \hat{t}^\dagger \hat{g}_R^R \hat{t} \hat{G}_d^R(\omega) [\hat{g}_d^{-1}(\omega)]^K \hat{G}_d^A(\omega) \right] \\
&\quad - \frac{1}{2} \text{Tr} \left[-\hat{t}^\dagger \hat{G}_d^R(\omega) ([\hat{g}_d^R(\omega)]^{-1} - [\hat{g}_d^A(\omega)]^{-1}) \hat{G}_d^A(\omega) \hat{t} \hat{g}_L^A + \hat{t} \hat{g}_L^R \hat{t}^\dagger \hat{G}_d^R(\omega) ([\hat{g}_d^R(\omega)]^{-1} - [\hat{g}_d^A(\omega)]^{-1}) \hat{G}_d^A(\omega) \right. \\
&\quad \left. + \hat{t} \hat{G}_d^R(\omega) ([\hat{g}_d^R(\omega)]^{-1} - [\hat{g}_d^A(\omega)]^{-1}) \hat{G}_d^A(\omega) \hat{t}^\dagger \hat{g}_R^A - \hat{t}^\dagger \hat{g}_R^R \hat{t} \hat{G}_d^R(\omega) ([\hat{g}_d^R(\omega)]^{-1} - [\hat{g}_d^A(\omega)]^{-1}) \hat{G}_d^A(\omega) \right] [1 - 2n(\omega)].
\end{aligned} \tag{C8}$$

The direct calculation shows

$$\text{Tr} \left[-\hat{t}^\dagger \hat{G}_d^{R(A)} \hat{t} \hat{g}^{R(A)} + \hat{t} \hat{g}^{R(A)} \hat{t}^\dagger \hat{G}_d^{R(A)} \right] = 0, \quad (\text{C9})$$

$$\text{Tr} \left[-\hat{t} \hat{G}_d^{R(A)} \hat{t}^\dagger \hat{g}^{R(A)} + \hat{t}^\dagger \hat{g}^{R(A)} \hat{t} \hat{G}_d^{R(A)} \right] = 0, \quad (\text{C10})$$

which implies that $I_{S,c}$ vanishes. This result shows that the spin current is fully induced by the term associated with the dissipation effect. Thus, the spin current is expressed as

$$I_S = I_{S,uc}. \quad (\text{C11})$$

-
- [1] A. Barone and G. Paterno, *Physics and applications of the Josephson effect* (Wiley, 1982).
- [2] D. Vollhardt and P. Wolfe, *The superfluid phases of helium 3* (Courier Corporation, 2013).
- [3] M. Nitta, Josephson junction of non-abelian superconductors and non-abelian josephson vortices, Nuclear Physics B **899**, 78 (2015).
- [4] C. J. Pethick and H. Smith, *Bose–Einstein condensation in dilute gases* (Cambridge university press, 2008).
- [5] R. Fagaly, Superconducting quantum interference device instruments and applications, Review of scientific instruments **77** (2006).
- [6] M. Kjaergaard, M. E. Schwartz, J. Braumüller, P. Krantz, J. I.-J. Wang, S. Gustavsson, and W. D. Oliver, Superconducting qubits: Current state of play, Annual Review of Condensed Matter Physics **11**, 369 (2020).
- [7] A. A. Golubov, M. Y. Kupriyanov, and E. Il’ichev, The current-phase relation in josephson junctions, Rev. Mod. Phys. **76**, 411 (2004).
- [8] A. O. Caldeira and A. J. Leggett, Influence of dissipation on quantum tunneling in macroscopic systems, Phys. Rev. Lett. **46**, 211 (1981).
- [9] J. Baselmans, A. Morpurgo, B. Van Wees, and T. Klappwijk, Reversing the direction of the supercurrent in a controllable josephson junction, Nature **397**, 43 (1999).
- [10] L. Bulaevskii, V. Kuzii, and A. Sobyenin, Superconducting system with weak coupling to the current in the ground state, JETP Lett.(USSR)(Engl. Transl.);(United States) **25** (1977).
- [11] V. B. Geshkenbein, A. I. Larkin, and A. Barone, Vortices with half magnetic flux quanta in “heavy-fermion” superconductors, Phys. Rev. B **36**, 235 (1987).
- [12] V. V. Ryazanov, V. A. Oboznov, A. Y. Rusanov, A. V. Veretennikov, A. A. Golubov, and J. Aarts, Coupling of two superconductors through a ferromagnet: Evidence for a π junction, Phys. Rev. Lett. **86**, 2427 (2001).
- [13] D. J. Van Harlingen, Phase-sensitive tests of the symmetry of the pairing state in the high-temperature superconductors—evidence for $d_{x^2-y^2}$ symmetry, Rev. Mod. Phys. **67**, 515 (1995).
- [14] J.-P. Cleuziou, W. Wernsdorfer, V. Bouchiat, T. Ondarçuhu, and M. Monthieux, Carbon nanotube superconducting quantum interference device, Nature nanotechnology **1**, 53 (2006).
- [15] T. Yamashita, K. Tanikawa, S. Takahashi, and S. Maekawa, Superconducting π qubit with a ferromagnetic josephson junction, Phys. Rev. Lett. **95**, 097001 (2005).
- [16] S. Krinner, T. Esslinger, and J.-P. Brantut, Two-terminal transport measurements with cold atoms, Journal of Physics: Condensed Matter **29**, 343003 (2017).
- [17] D. Husmann, S. Uchino, S. Krinner, M. Lebrat, T. Giamarchi, T. Esslinger, and J.-P. Brantut, Connecting strongly correlated superfluids by a quantum point contact, Science **350**, 1498 (2015).
- [18] G. Valtolina, A. Burchianti, A. Amico, E. Neri, K. Khani, J. A. Seman, A. Trombettoni, A. Smerzi, M. Zaccanti, M. Inguscio, *et al.*, Josephson effect in fermionic superfluids across the bec-bcs crossover, Science **350**, 1505 (2015).
- [19] S. Levy, S. levy, e. lahoud, i. shomroni, and j. steinhauer, nature (london) 449, 579 (2007)., Nature (London) **449**, 579 (2007).
- [20] W. Kwon, G. Del Pace, R. Panza, M. Inguscio, W. Zwirger, M. Zaccanti, F. Scazza, and G. Roati, Strongly correlated superfluid order parameters from dc josephson supercurrents, Science **369**, 84 (2020).
- [21] G. Del Pace, W. J. Kwon, M. Zaccanti, G. Roati, and F. Scazza, Tunneling transport of unitary fermions across the superfluid transition, Phys. Rev. Lett. **126**, 055301 (2021).
- [22] F. Schäfer, T. Fukuhara, S. Sugawa, Y. Takasu, and Y. Takahashi, Tools for quantum simulation with ultracold atoms in optical lattices, Nature Reviews Physics **2**, 411 (2020).
- [23] L. Corman, P. Fabritius, S. Häusler, J. Mohan, L. H. Dogra, D. Husmann, M. Lebrat, and T. Esslinger, Quantized conductance through a dissipative atomic point contact, Phys. Rev. A **100**, 053605 (2019).
- [24] M.-Z. Huang, J. Mohan, A.-M. Visuri, P. Fabritius, M. Talebi, S. Wili, S. Uchino, T. Giamarchi, and T. Esslinger, Superfluid signatures in a dissipative quantum point contact, Phys. Rev. Lett. **130**, 200404 (2023).
- [25] Y. Ashida, Z. Gong, and M. Ueda, Non-hermitian physics, Advances in Physics **69**, 249 (2020).
- [26] C.-A. Li, H.-P. Sun, and B. Trauzettel, Anomalous andreev spectrum and transport in non-hermitian josephson junctions, Phys. Rev. B **109**, 214514 (2024).
- [27] J. Cayao and M. Sato, Non-hermitian phase-biased josephson junctions, Phys. Rev. B **110**, L201403 (2024).
- [28] P.-X. Shen, Z. Lu, J. L. Lado, and M. Trif, Non-hermitian

- fermi-dirac distribution in persistent current transport, Phys. Rev. Lett. **133**, 086301 (2024).
- [29] D. M. Pino, Y. Meir, and R. Aguado, Thermodynamics of non-hermitian josephson junctions with exceptional points, arXiv preprint arXiv:2405.02387 (2024).
- [30] C. W. J. Beenakker, Josephson effect in a junction coupled to an electron reservoir, Applied Physics Letters **125**, 122601 (2024), <https://pubs.aip.org/aip/apl/article-pdf/doi/10.1063/5.0215522/20158679/122601.1.5.0215522.pdf>.
- [31] J. Cayao and M. Sato, Non-hermitian multiterminal phase-biased josephson junctions, Phys. Rev. B **110**, 235426 (2024).
- [32] R. Capecelatro, M. Marciani, G. Campagnano, and P. Lucignano, Andreev non-hermitian hamiltonian for open josephson junctions from green's functions, Phys. Rev. B **111**, 064517 (2025).
- [33] D. C. Ohnmacht, V. Wilhelm, H. Weisbrich, and W. Belzig, Non-hermitian topology in multiterminal superconducting junctions, Phys. Rev. Lett. **134**, 156601 (2025).
- [34] A. Sten, P. Dutta, and S. K. Ghosh, Angle-dependent dissipation effects in topological insulator-based josephson junctions, arXiv preprint arXiv:2502.09397 (2025).
- [35] H.-P. Breuer and F. Petruccione, *The theory of open quantum systems* (Oxford University Press, USA, 2002).
- [36] A. J. Daley, Quantum trajectories and open many-body quantum systems, Advances in Physics **63**, 77 (2014).
- [37] A.-M. Visuri, J. Mohan, S. Uchino, M.-Z. Huang, T. Esslinger, and T. Giamarchi, Dc transport in a dissipative superconducting quantum point contact, Phys. Rev. Res. **5**, 033095 (2023).
- [38] We assume that tunneling occurs between the position $\mathbf{r} = \mathbf{0}$ in each reservoir and the quantum dot. Therefore, $\psi_{L(R)\sigma}$ is the shorthand notation of $\psi_{L(R)\sigma}(\mathbf{0})$.
- [39] S. Uchino, Comparative study for two-terminal transport through a lossy one-dimensional quantum wire, Phys. Rev. A **106**, 053320 (2022).
- [40] A. Kamenev, *Field theory of non-equilibrium systems* (Cambridge University Press, 2011).
- [41] L. M. Sieberer, M. Buchhold, and S. Diehl, Keldysh field theory for driven open quantum systems, Reports on Progress in Physics **79**, 096001 (2016).
- [42] J. C. Cuevas, A. Martín-Rodero, and A. L. Yeyati, Hamiltonian approach to the transport properties of superconducting quantum point contacts, Phys. Rev. B **54**, 7366 (1996).
- [43] A. Martín-Rodero and A. Levy Yeyati, Josephson and andreev transport through quantum dots, Advances in Physics **60**, 899 (2011).
- [44] B. J. van Wees, K.-M. H. Lenssen, and C. J. P. M. Harmans, Transmission formalism for supercurrent flow in multiprobe superconductor-semiconductor devices, Phys. Rev. B **44**, 470 (1991).
- [45] P. Samuelsson, J. Lantz, V. S. Shumeiko, and G. Wendin, Nonequilibrium josephson effect in mesoscopic ballistic multiterminal junctions, Phys. Rev. B **62**, 1319 (2000).
- [46] A. Martín-Rodero, A. L. Yeyati, and J. Cuevas, Transport properties of normal and ferromagnetic atomic-size constrictions with superconducting electrodes, Physica C: Superconductivity **352**, 67 (2001).
- [47] M. Kohda, S. Nakamura, Y. Nishihara, K. Kobayashi, T. Ono, J.-i. Ohe, Y. Tokura, T. Mineno, and J. Nitta, Spin-orbit induced electronic spin separation in semiconductor nanostructures, Nature communications **3**, 1 (2012).
- [48] R. Labouvie, B. Santra, S. Heun, and H. Ott, Bistability in a driven-dissipative superfluid, Phys. Rev. Lett. **116**, 235302 (2016).
- [49] J. Rammer, *Quantum field theory of non-equilibrium states* (Cambridge University Press, 2007).
- [50] H. Haug, A.-P. Jauho, *et al.*, *Quantum kinetics in transport and optics of semiconductors*, Vol. 2 (Springer, 2008).